A new adhesively bonded composite repair for offshore steel structures: strength assessment and fatigue

Quentin Sourisseau, Emilie Lepretre, Sylvain Chataigner, Xavier Chapeleau, Maxime Deydier, Stéphane Paboeuf

CICE 2023 Rio de Janeiro – Brazil 11TH INTERNATIONAL CONFERENCE ON FRP COMPOSITES IN CIVIL ENGINEERING

A NEW ADHESIVELY BONDED COMPOSITE REPAIR FOR OFFSHORE STEEL STRUCTURES: STRENGTH ASSESSMENT AND FATIGUE

Quentin Sourisseau MAST-SMC, COSYS-SII, I4S Team (Inria)
Université Gustave Eiffel, France, Bureau Veritas Marine & Offshore, Research Department, France
quentin.sourisseau@univ-eiffel.fr
Emilie Lepretre MAST-SMC, Université Gustave Eiffel, Bouguenais, France emilie.lepretre@univ-eiffel.fr
Sylvain Chataigner MAST-SMC, Université Gustave Eiffel, Bouguenais, France,
sylvain.chataigner@univ-eiffel.fr
Xavier Chapeleau COSYS-SII, I4S Team (Inria), Université Gustave Eiffel, Bouguenais, France,
xavier.chapeleau@univ-eiffel.fr
Maxime Deydier Bureau Veritas Marine & Offshore, Research Department, Saint Herblain, France,
maxime.deydier@bureauveritas.com
Stéphane Paboeuf Bureau Veritas Marine & Offshore, Research Department, Saint Herblain,
France, stephane.paboeuf@bureauveritas.com

ABSTRACT

Floating productions, storage and offloading (FPSO) units are subject to corrosion problems. The use of adhesively bonded FRP patches as a repair appears to be a particularly interesting solution. However, design strategies still need to be improved and validated to insure the robustness and, ultimately, confidence in this solution. Since 2018, Bureau Veritas leads a joint industrial project called Strength Bond Offshore which aims at defining such a design strategy. First, the patch designed during this project will be presented. Then, the experimental test campaign is detailed: manufacturing, monotonic tests in traction and bending. Finally, the results of the fatigue tests campaign are developed. Ongoing additional developments are under progress to better assess equivalent interfacial behaviors for an overall design strategy.

Keywords: Bonding, Offshore, Reinforcement, Optical fiber sensor

INTRODUCTION

Corrosion of metallic structures in an offshore environment is an ongoing threat due to high temperature and humidity conditions, especially in tropical environments. A bonded repair of these corroded surfaces has several advantages, including short downtime and a non-intrusive repair process. However, repairing corroded areas on large marine structures by bonding FRP patches imposes significant constraints on the design. The patch end is placed in a fully stressed zone (zone subject to unit bending), causing high stresses on the edges of the reinforcement. More generally, designers and engineers have to deal with several difficulties related to the nature of steel-composite assemblies: discontinuity of materials (different properties of materials), nonlinear material properties of the adhesive, singularity constraint at the edges of the patch. A fine understanding of adhesion mechanics and patch strength are essential for designing highly reliable composite repairs. These difficulties of design tend to greatly limit the industrial applications of bonded reinforcements, particularly in an offshore environment. However, it has been proven in the laboratory that these types of reinforcements can have very beneficial effects on the service life of reinforced structures (Chataigner et al.,2018; Chataigner et al., 2020; Leprêtre et al., 2018).

A Joint Industrial Project (JIP) called "Strength Bond Offshore" (SBO) was thus initiated (Bureau Veritas 2020), in order to:

- validate a characterization procedure for the components of the bonded assembly,
- standardize the qualification process for bonded composite repairs in an offshore environment,

• define a robust method for predicting the resistance of the bonded patch,
• enable a clear assessment of the safety factor to be taken into account in the estimation of design loads.
The work presented in this article aims at complying with this last goal. First, the design of the composite patch (carbon fibers/glass fibers/epoxy resin) developed during the SBO project will be detailed by Paboeuf (2021). The studied solution is based on the production and bonding of composite patches by infusion, with a dedicated surface preparation protocol. The preliminary investigations made on all specimens and carried out using fracture mechanics for the dimensioning of the bonded patch are presented in detail by Sourisseau (2022) and Sourisseau et al. (2022). Only a few significant results will be recalled in this article. To validate the design of the bonded patch, full size specimens were also tests under monotonic loading (traction/bending), as well as fatigue tests (traction) were carried out with full-scale specimens. The obtained results are compared with predictive calculations for typical loading cases encountered on FPSO units.

PATCH DESIGN PRESENTATION

The loads applied to the hull of a ship are mainly related to the effect of the waves and to the loadings of the ship (loads in calm water). Since a ship has a significant length compared to its width and depth, it can be considered as a beam element and is thus submitted to vertical/horizontal bending moment (generated by waves) and shear/bending loads (generated by the vessel's own weight). These induce a large amplitude of in-plane stresses (traction, compression, shear) for the longitudinal elements of the structure: hull and partitions. For wave loads, a Weibull distribution law is defined in Bureau Veritas rules for steel vessels (NR467, 2022) and rules for offshore units (NR445, 2022), with data from guidelines for fatigue assessment of steel vessels and offshore units (NI611, 2020). Within the framework of the dimensioning of a bonded reinforcement of large dimensions, only the global loads of the ship beam are taken into account. They can be summarized as follows (loads due to waves and loads in calm water):

- tensile/compressive loads in steel s_{xx} =+/-225 MPa,
- shear load in steel τ_{xy} = 45 MPa.

Note that these values correspond to an extreme loading case for a ship in its original condition (uncorroded), with a probability level of 10^{-8}.

The bonded patch must therefore satisfy these resistance criteria while guaranteeing maximum rigidity to regain the lost stiffness of the structure caused by corrosion. As part of this study, the loss of steel thickness to be recovered by the composite patch was evaluated to be equal to approximately 7 mm for a 20 mm thick sheet (30% loss). The design of the bonded patch, under these conditions, led to a proposal for composite layup detailed in Figure 1. Two types of angles (long and short scarfs) at the edges of the patch are proposed and the influence of the variation of this angle (stresses concentrations) on the resistance of the patch is studied. Each stack of unidirectional plies is represented by a color in Figure 1. The grey/blue/black colored layers correspond to the thirty-six carbon fibers plies at a given angle (from 0° to 90°). The green layers represent plies of glass fibers oriented at 0°/90°. Finally, the orange layer corresponds to the steel substrate. It should be noted that the two upper fiberglass plies are only there to protect the carbon part of the patch from external aggressions.

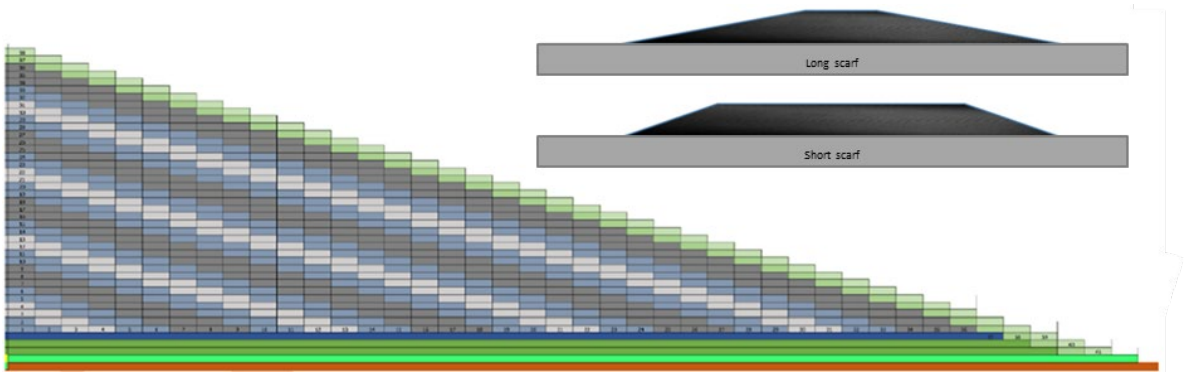

Figure 1: Layup of the bonded patch and studied scarfs geometries.

MANUFACTURING

The chosen manufacturing process for the realization of the different bonded patches is based on the method of impregnation by infusion with surface preparation defined for the project (Sourisseau, 2022; Sourisseau et al., 2022). Figure 2 shows the stacking process of the different plies before infusion. The used resin is a post-cured epoxy resin (80°C for 16 hours). In order to obtain more information on the mechanical state of the patch during the various tests, optical fiber sensors, for measuring distributed strain, were placed inside the patch for the allthe samples (between the first two plies of glass fibers, close to the surface with the steel) as well as on the surface of the patch for all samples (figure 3). These fibers are polyimide distributed optical fibers that allow a spatial resolution of 1,2mm with noise measurement of $\pm 20\%$ µstrain, paired with an Luna Odisi-b interrogator. The steel sheet has a high elastic limit (900 MPa) to guarantee the absence of yielding before the patch peels off. The produced large specimens (real scale) are then cut with a water jet. The dimensions of the resulting specimens are 2000 mm long and 50 mm wide. The bonded patch is about 1400 mm long, leaving a free length on each side of 300 mm (Figure 4).

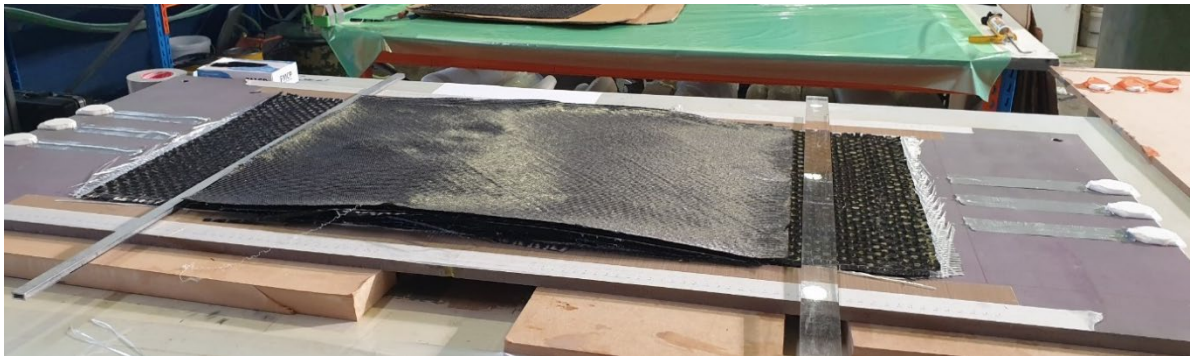

Figure 2: Plies stacking before infusion with embedded optical fibers in the patch.

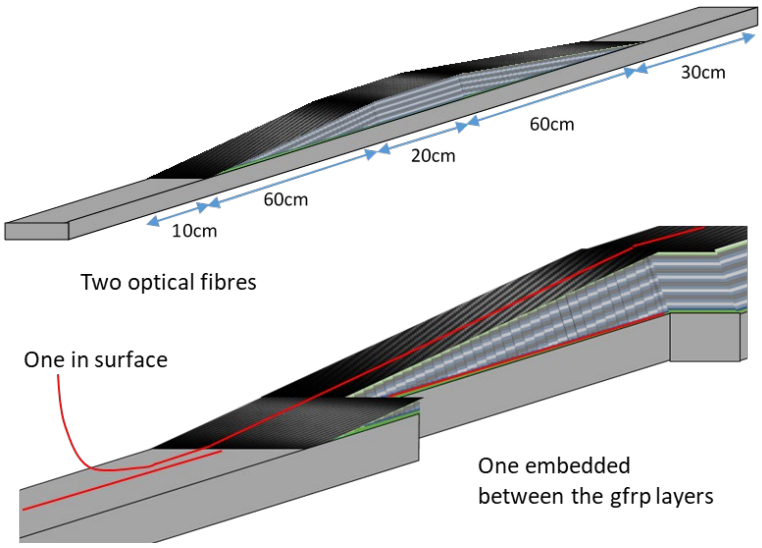

Figure 3: Instrumentation, optical fiber position and sample size, long scarf sample example.

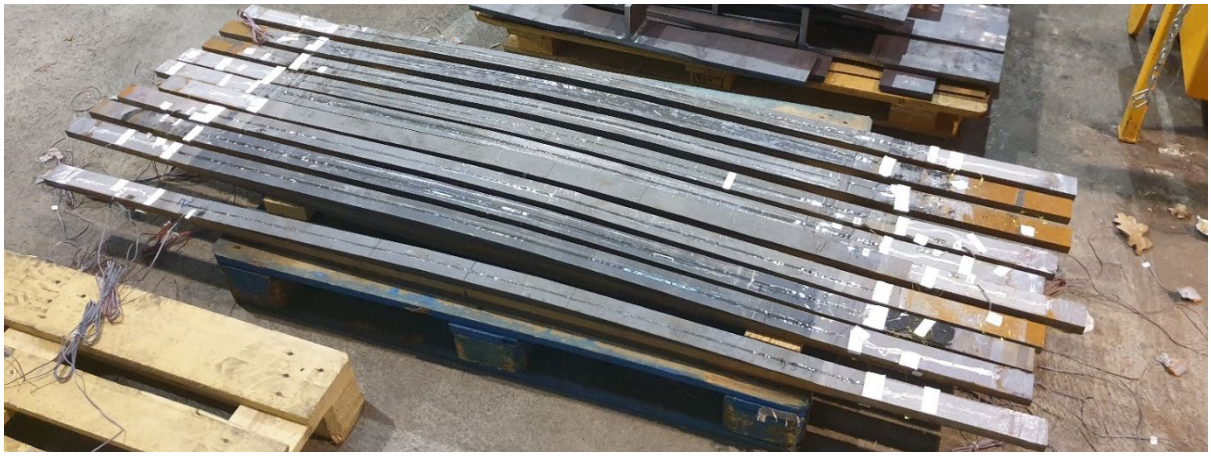

Figure 4: Samples after water jet cutting.

After cutting, the observation of the specimens showed that some porosities exist in the central part of the patch (the thickest). Their position being in the least mechanically loaded zone makes it possible to limit their influence on the mechanical properties of the patch. The after-test analysis of the sample proved that they were the only defect in and on the samples.

STRENGTH ASSESSMENT OF THE BONDED PATCH UNDER MONOTONIC STRESS

Figure 5 presents the two types of static tests carried out during our investigations. On the left, a tensile test is carried out on an Instron tensile machine with an ultimate capacity of 2500 kN while on the right, 3 points bending test is carried out on a Losen press with a capacity of 300 kN. The distances between supports for the bending test are 1450 mm. These two tests were chosen because they were identified as similar two the two types of solicitation that the patches would encounter in real case application.

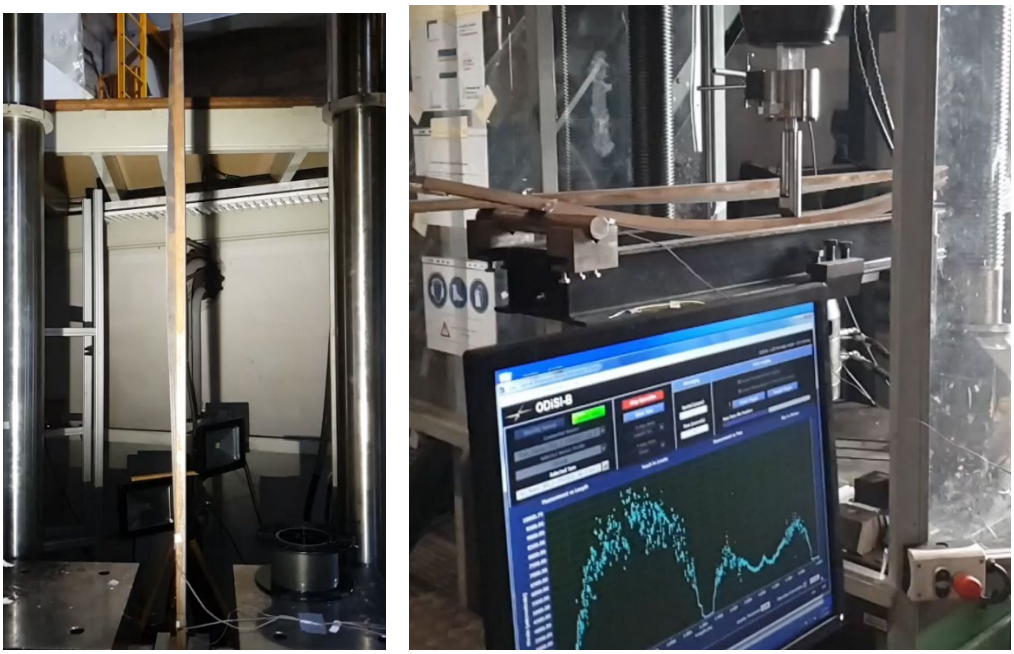

a) *b)*

Figure 5: Traction (a) and three points bending (b) tests of composite to steel bonded assembly patch.

These tests are made to measure the ultimate states at failure (strain) in the bonded patches as well as the ultimate capacities (force) for the two types of scarfs (short and long) and for the two types of tests

(traction and bending). Table 1 summarizes the ultimate forces obtained in each case. The observed failure behavior is purely brittle with linear elastic loading until sudden and total debonding of the patch. For specimens with a short scarf, the average failure load in tension is 489 kN and, in bending, is 34 kN. The results are weakly dispersed. Taking into account the steel part of the specimens (50 mm wide x 20 mm thickness), it is possible to calculate an equivalent stress in the steel for a reinforced sheet. This value is 490 MPa for an ultimate capacity of 489 kN, this corresponds to more than the double of what is recommended by Bureau Véritas design rules (490 MPa versus 225 MPa).
Tests on specimens with a long scarf show greater failure load in tension, in the order of 787 kN on average (+60% compared to specimens with a short scarf) and similar forces (slightly lower) in the case of bending. For the studied specimen geometries, these results tend to demonstrate that the impact of the scarf length in bending is very limited, whereas in tension, it allows a clear improvement in the maximum resistance of the bonded patch. These results are related to the different strain profiles depending of the different solicitations. The three points bending test being more loaded on the center position of the patch (smaller strain gradient at the border than for tension test), failure load are less dependent of the scarf angles.

Table 1: Failure loads obtained for the samples with long and short scarf.

	Long scarf		Small scarf	
Failure load	Tension (kN)	Bending (kN)	Tension (kN)	Bending (kN)
Test 1	840	32	477	35
Test 2	790	29	500	31
Test 3	795	30	491	36
Test 4	740	29		
Test 5	769			
Average	787	30	489	34
Standard deviation/average	3%	3%	2%	8%

The experimental results were compared with the results obtained for a bonded steel sheet solution having similar geometries as the composite specimen (Sourisseau et al., 2022). These results are summarized in Table 2. They highlight a clear gain with respect to the forces at break in the case of a repair by bonded composite patch compared to a similar repair (equivalent stiffness) using a steel sheet (6 mm thick). These results therefore indicate that for a real application, the choice of the large scarf will allow better performance of the bonded composite patch with a safety factor of approximately 3.5 (790 MPa vs 225 MPa) on the admissible breaking stresses in the steel before patch debonding (NI611).

Table 2: Average stress in steel at failure for three different bonded repair configurations of an equivalent thickness.

Type of bonded reinforcement	Equivalent stress in steel (MPa, in tension)
Short scarf composite patch	495
Long scarf composite patch	787
Steel patch	250

Figure 6 shows the obtained fracture surfaces after the tensile tests for specimens with a long scarf. A multi-interfacial rupture is observed between the steel and the resin, the first ply of glass fibers and the resin, as well as the beginning of delamination between the first two plies of glass fibers (white area on the patch). Similar fracture surfaces were obtained for the two types of scarfs, as well as for the two types of tests (tension and bending), showing a similar failure mode. The low dispersion of the ultimate forces, combined with similar fracture surfaces, is yet a guarantee of repeatability and confidence in the overall behavior of the patch.

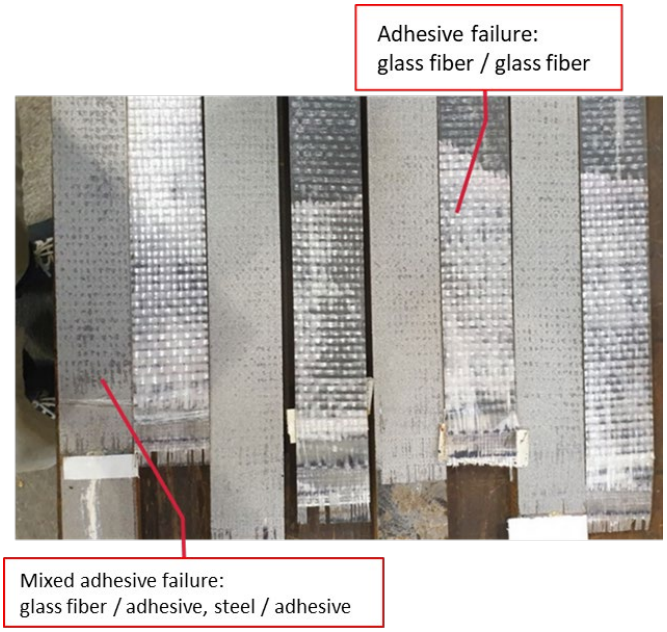

Figure 6: Fracture surfaces of tested samples in tension with long scarf.

EFFECT OF THE PATCH DESIGN ON INTERNAL STRAINS

Bending Test

As exposed before, to obtain more information on the mechanical state of the patch and to validate that the stress concentration at the border of the patch is limited by the design, distributed strain measurements have been recorded during the tests. A high-definition optical fiber sensing system (based on the Rayleigh backscattering) with sub-millimeter sampling resolution was used for the measurements. This system has a maximum sampling rate of approximately 20 Hz and, for the post-processing of data, the gauge length and spacing were fixed to be equal to 1 mm.

The Figure 7 presents the obtained strains measurement along the optical fiber for one of the bending test with a specimen with small scarfs.

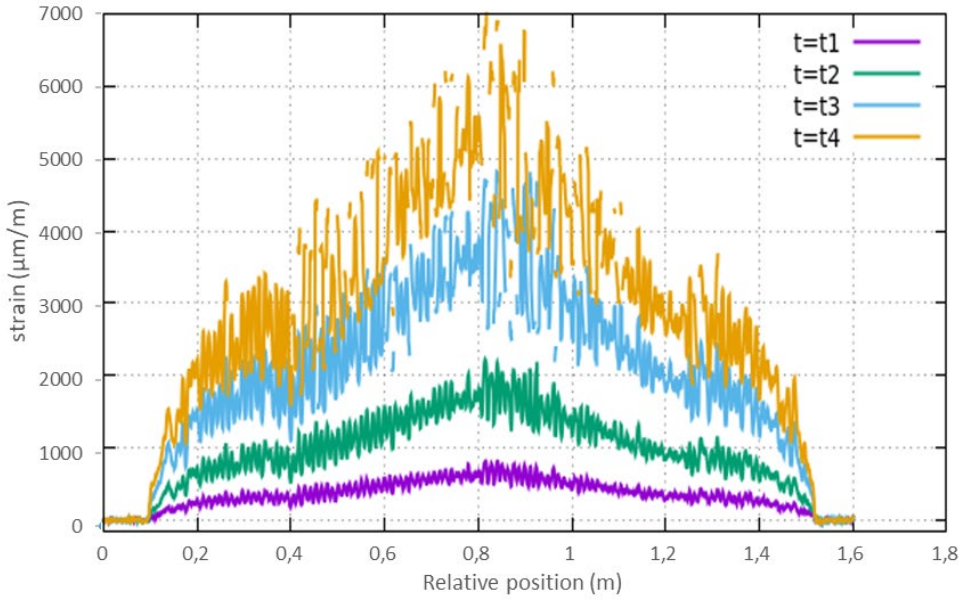

Figure 7: Bending test of small scarf samples optical fiber surface strains measurement.

Figure 8 presents an example of the strain measurement obtained by the distributed optical fiber sensor during the bending test for a specimen with long scarfs. For all the figures, the abscise represent the relative position of the optical fiber on the patch (1.4m length patch). Embedded fiber measurements for small scarf samples are not provided, because the fibers were broken during the water jet cutting of the samples. The left part of the curves shows the surface measurement and right part of the curves the embedded one. For all the described results, the time t_4 corresponds to the last strains measurement before the failure of the patch and time t_1, t_2 and t_3 correspond to time during the loading of the patch.

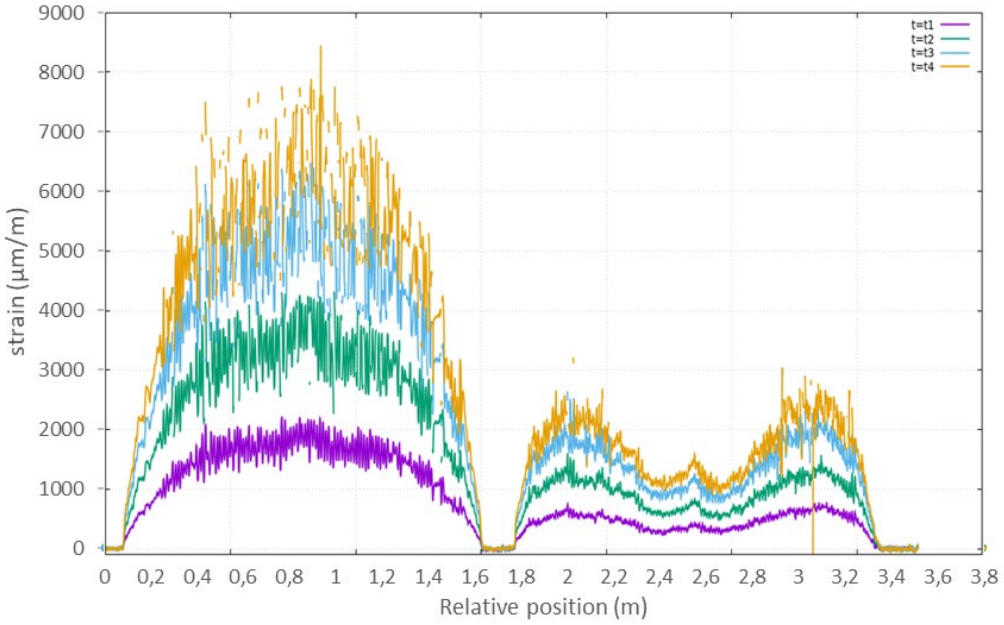

Figure 8. Bending test of long scarf samples optical fiber outside (left) and inside (right) strains measurement.

For the bending test (figures 7 and 8), the observation of strains profile on the surface of the patches shows that no strains concentrations are visible at the border of the patch (whether it be for the small scarfs or the long scarfs samples). In the case of the long scarf sample with embedded fiber, the direct effect of the patch on the steel surface strains is visible. It can be seen that they remain really low, especially in the center section of the patch. It indicates that the patch help to reduce stress in the steel surface where it is supposed to be corroded

Tension Test

The figure 9 presents the strains measurement obtained along the patch for one of the small scarfs specimens tested in tension. While, figure 10 presents the measured distributed strains during the tension test for a long scarfs sample. The left part of the curves shows the surface measurement and right part of the curves, the embedded one.

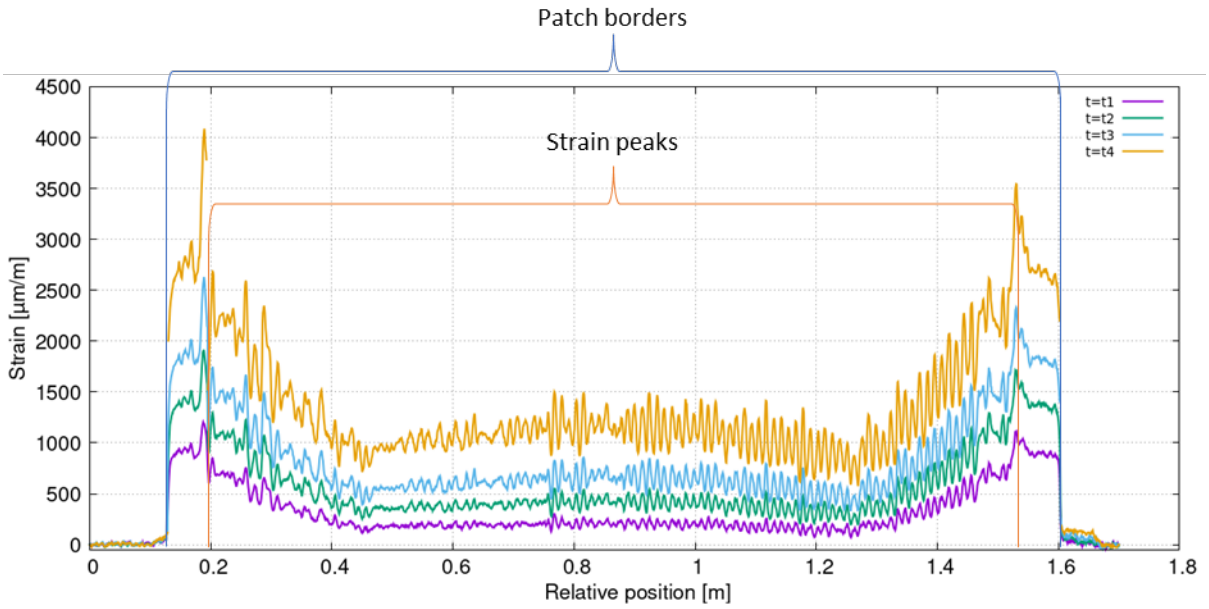

Figure 9: Tension test of small scarf sample optical fiber surface strain measurement.

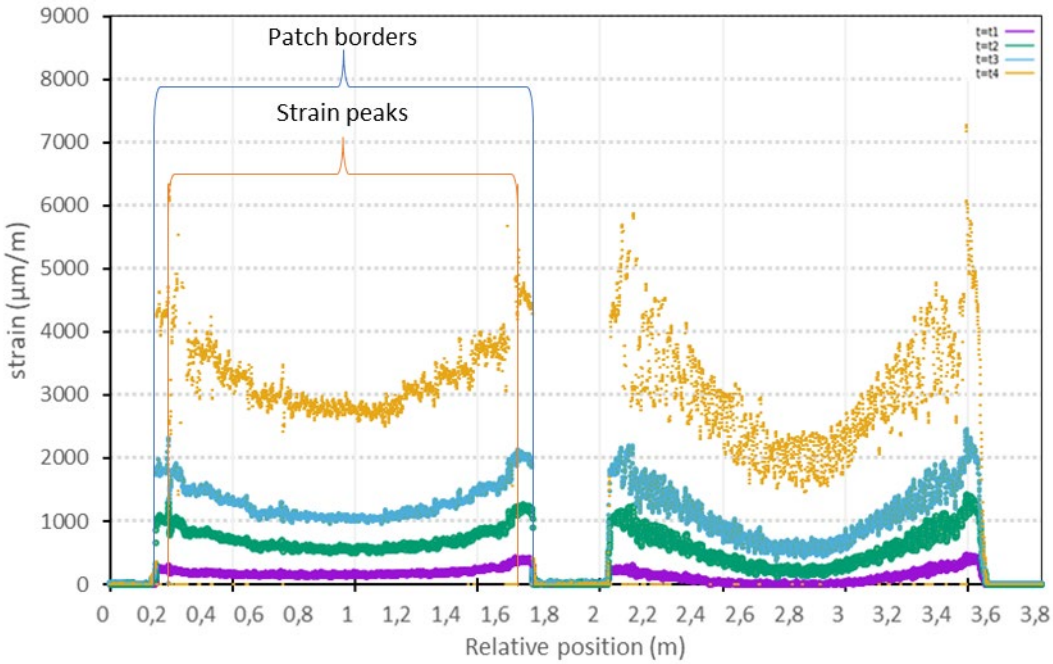

Figure 10: Tension test of long scarf sample, optical fiber inside (left) and outide (right) strains measurement.

For the tension test, two high strain peaks are clearly visible between 5 and 7 cm from the border of the patch (figure 9 and figure 10). These locations correspond to the position of the border of the first carbon plies. When comparing the small scarf surface results (figure 9) and long scarf surface (figure 10), the strain transition length (distance of the effect of scarf from the border of the patch) is much longer for the long scarf. It allows to obtain locally, higher strain at failure. From the results of the embedded optical fiber, it can be seen than, compare to the short scarf results, the strain gradient is much lower at failure. It indicates that the longer scarf allows to have a much smoother strain transition from the steel plate to the patch. Also, these results indicates that despite the capacity of the patch to sustain equivalent strain in the steel plate of around 787MPa for the long scarf, ultimate properties could be increased by further modification of the design (example: change in the layup to reduce the strain peak at the patch border). These results also prove that the patch performances (much higher than the standard requirement) are directly linked to the patch design. The tension test seems to be more critical because

of the much higher strain gradient near the patch borders. This conclusion as led to the choice to limit the fatigue test campaign (described in the next chapter) to only tension tests.

Composites patch fatigue behavior assessment

To assess the behavior of the composite patch in fatigue, 10 tensile tests were carried out. From the results of the static tests on specimens with a long scarf, different load levels in traction, with a load ratio $R=\sigma_{max}/\sigma_{min} = 0.1$ have been chosen for the tests. The number of cycles at failure vary with applied load, between 50,000 and 5 million of cycles. Figure 11 shows the results of these tests in terms of service life, for different amplitudes of force. The orange squares correspond to the test results (at break), and the blue arrows to the tests which have not broken for a number of cycles corresponding to the base of the arrow. From these points of measurements, the fatigue curve is plotted in the figure (black straight line). For comparison, the fatigue curve of a reference FPSO unit calculated from the NI611 (2020) standard is also shown in the figure. It can thus be seen that the service life of the patch, obtained for different load amplitudes, is much greater than that of the reference histogram (minimum theoretical service life of the ship for each possible load level).

Moreover, the number of cycles undergone during the life of a reference FPSO unit can be calculated from the formula given in Eq. 1. A target lifetime of 20 years corresponds to 63 million cycles. This value is reported in the figure 11 (vertical blue line).

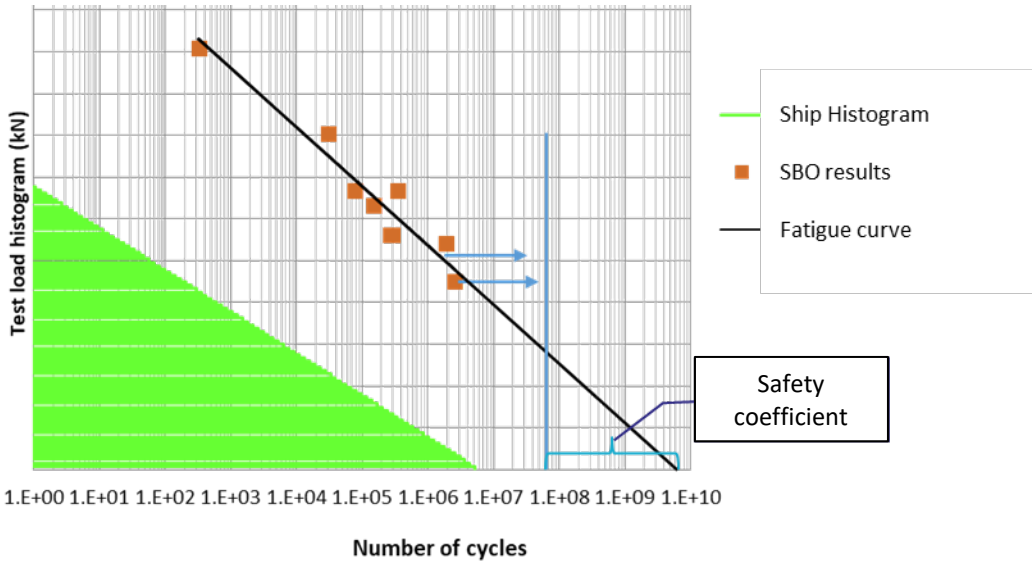

Figure 11. Results obtained from the fatigue test campaign in tension on long scarf samples.

$$N_{cycles} = D_{life} F_{wave} \qquad \text{Eq. 1}$$

With N_{cycles} corresponding to the number of cycles at failure, D_{life} the expected lifetime and F_{wave} to the average wave frequency, here fixed at 0.1Hz.

These results therefore predict that the lifetime of the patch, in real conditions of use and without external damage, will greatly exceed the lifetime of the ship. The high safety factor (difference between the theoretical and experimental lifespan) provides a very good level of confidence in the behavior of the bonded patch in real conditions.

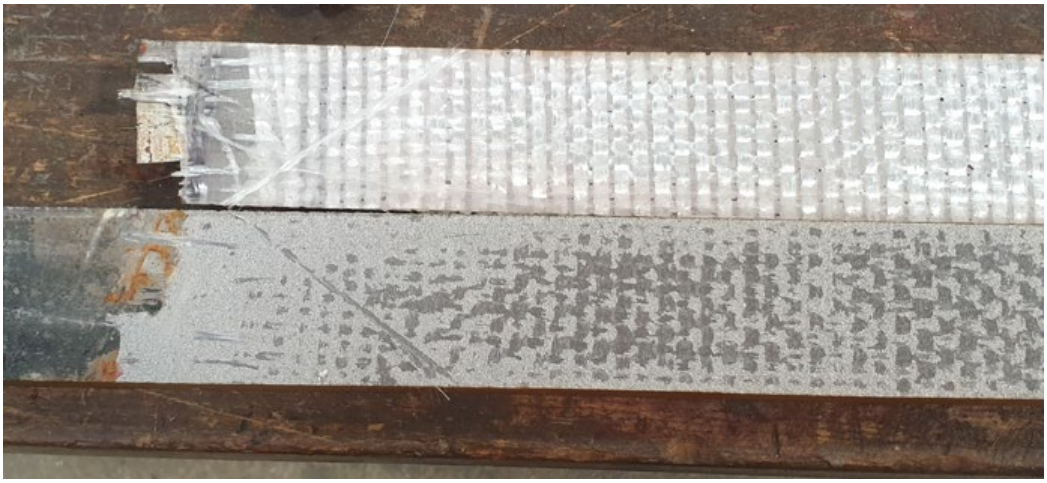

Figure 12. Fracture surfaces of the fatigue test samples in tension.

The Figure 12 shows the obtained fracture surfaces after the fatigue tensile tests A multi-interfacial failure similar the ones obtained for the monotonic test has been observed. Similar fracture surfaces were obtained for all the load level tested. It is concluded that when a fatigue crack is initiated in the patch, the failure of the patch occurs in the same way as in the monotonic test and therefore, no real fatigue crack propagation happened. This assumption has been validated by the witnessing of the violented debonding of the patch during fatigue tests.

Conclusion

An adhesively bonded composite patch was developed during the SBO project and was detailed. It consists in an infused composite patch (ply-stacking) associated with a dedicated surface preparation and a post-cure cycle feasible on site. To assess the performance of the developed patch, full-scale investigations were realized and are presented.

Those consisted in evaluating the resistance of the bonded patch for several types of monotonous loading (traction and bending). These tests have shown the very good mechanical performance of the patch designed in the SBO project, being two to three times higher (depending on the angle of the scarf) than the values recommended by the standards. In addition, a specific monitoring strategy (use of continuous optical fiber) was used to better understand the importance of the edge treatment on the obtained results. Good repeatability and similar failure modes were obtained indicating the robustness of the developed protocol and the consistency of a dedicated design approach.

In addition, the results of the fatigue test campaign have shown that the lifetimes under fatigue loading are much higher than the design loadings of an FPSO unit. These results are very promising for the use of bonded composite patches as a means of reinforcing corroded sheets in an offshore environment. Additional developments are under progress to propose an equivalent interfacial approach suitable to be used for the design of such patches.

Yet, these results do not take into account the possible external degradation of the patch caused by humidity or the possible damage following an impact. The loss of mechanical performance resulting from these various degradations will further be studied to guarantee the proper functioning of the bonded composite patch as a durable reinforcement for the FPSO unit.

ACKNOWLEDGEMENTS

Acknowledgments to project partners StrengthBond Offshore (Bureau Veritas, Total, Petrobras, Naval Group, Siemens, ColdPad et Infracore Compagny) who funded this work.

REFERENCES

Chataigner, S., Benzarti, K., Foret G., Caron, J.F., Gemignani, G., Brugiolo, M., Calderon, I., Pinero, I., Birtel, V., Lehmann, F., (2018). *Design and evaluation of an externally bonded CFRP reinforcement for the fatigue reinforcement of old steel structures*, Engineering Structures, Vol. 177, pp. 556-565.

Chataigner, S., Wabeh, M., Garcia-Sanchez, D., Benzarti, K., Birtel, V., Fischer, M., Sopena, L., Boundouki, R., Lehmann, F., Martin, E., Gemignani, G., Zalbide, M., (2020). *Preventive fatigue strengthening of steel structures with adhesively bonded CFRPs – efficiency demonstration on a real bridge*, Journal of Composites for construction, 24 (3).

Lepretre, E., Chataigner, S., Dieng, L., Gaillet, L., (2018). *Fatigue strengthening of cracked steel plates with CFRP laminates in the case of old steel materials*, Construction and Building Materials, Vol. 174, pp. 421-432.

https://marine-offshore.bureauveritas.com/strength-bond-offshore-assessing-strength-bonded-repairs

Paboeuf, S., Sourisseau, Q., Goupil A-C., (2021). *Towards a Robust Offshore Bonded Repair Strength Evaluation*, SNAME 2021 - 26th Offshore Symposium. Houston Texas, USA, ISBN: 978-1-7138-3136-5

Sourisseau, Q., Lepretre, E., Chataigner, S., Chapeleau, X., Paboeuf, S., Deydier M., (2022). *Adhesively Bonded FRP Reinforcement of Steel Structures: Surface Preparation Analysis and Influence of the Primer*, ASME 2022 - 41st International Conference on Ocean, Offshore and Arctic Engineering, Hamburg, Germany, pp.1-9, doi: 10.1115/OMAE2022-79079.

Sourisseau, Q., *Development of a robust methodology for the design assessment of bonded reinforcements on steel structures*, Ph.D. thesis, Université Gustave Eiffel, Nantes Université, 2022.

NI467, Rules for the classification of steel ships, Jul 2022, Bureau Veritas

NI445, Rules for the classification of offshore units, Nov 2022, Bureau Veritas

NI611, Guidelines for fatigue assessment of ships and offshore units, Nov 2020, Bureau Veritas

CONFLICT OF INTEREST

The authors declare that they have no conflicts of interest associated with the work presented in this paper.

DATA AVAILABILITY

Data on which this paper is based is available from the authors upon reasonable request.